

# AN IMPLEMENTATION OF TRANSFORMER-LESS DYNAMIC VOLTAGE RESTORER

<sup>1</sup>S.RAMA LAKSHMI, <sup>2</sup>P.HEMANTH PRITHVI

<sup>1</sup>M.Tech Student, <sup>2</sup>Assistant Professor

Department of EEE

KAKINADA INSTITUTE OF TECHNOLOGICAL SCIENCES (KITS), RAMACHANDRAPURAM.

**Abstract:** A transformer-less dynamic voltage restorer (DVR) with bipolar voltage gain capability is proposed in this study. The DVR is formed by a three-leg ac/ac converter with its output capacitor in series with the transmission line. Since the energy used for voltage compensation is obtained from the grid, long-time voltage disturbances can be compensated without using bulky energy storage elements. As a result, the proposed DVR has the features of compact structure, light weight, and low cost. Moreover, it also has a high reliability as the commutation problem is avoided by adopting the proposed modulation strategy. A detailed analysis of the topology structure and operation principle is given, followed by the developed control method. Finally, simulations and experimental results are presented to verify the validity of the DVR.

**Keywords:** Dynamic Voltage Restorer, Voltage Sag, Voltage Swell, Z- Source AC-AC Converter

## 1. Introduction

Power quality (PQ) problems, such as voltage sags/swells and harmonics will cause malfunction of the equipment in the factories and disrupt the production processes, which lead to substantial economic losses [1–3]. Hence, they have emerged as a serious issue in industrial distribution systems. Different types of equipment are used to improve the PQ, e.g. dynamic voltage restorers (DVRs) [4, 5], active power filters [6–8] and uninterruptible power supplies [9].

As one of the most commonly used voltage compensators, DVR is preferred to tackle with the voltage-related PQ problems. Generally, the traditional DVR use a voltage source inverter (VSI) to generate the desired compensation voltage. Also, the input of the VSI is a stored energy element, such as massive capacitors, batteries or flywheels. Since the compensation capability of this type of restorer mainly depends on the capacity of the energy storage system, they are unable to compensate for the long duration voltage disturbances [10], whereas, DVR using the ac/ac converter does not encounter this issue [11] because the energy used for voltage compensation is dragged from the grid. According to the type of the ac/ac converter, they can be divided into direct ac/ac converter based DVR and indirect ac/ac converter based DVR.

The direct ac-ac converters can be buck, boost, or buck-boost type ac-ac converters [12, 13]; basic half-bridge, full-bridge, and push-pull converters [14]; direct matrix converter [15]; three-level ac/ac direct converter [16]; other types of derived or improved topologies [17–20]. They have the characteristics of simple topologies, no bulky energy storage components, small sizes, and low costs.

However, all direct ac-ac converters mentioned above present the typical commutation issue, since there are no passive elements and bi-directional switches have to be used. Addressing that, a variety of approaches have been investigated in [21–25]. They can be broadly classified into three kinds: (i) using resistor-capacitor snubbers to absorb the voltage spikes and allow a finite dead time in the gate signals [22, 23]; (ii) implementing soft commutation strategy to avoid the open-circuit of inductor current [24]; (iii) adopting the switching cell structure with coupled inductors [25]. Those may make them complex, costly, low efficient or unreliable in practical implementation.

Regarding the indirect ac/ac converter based DVR there is a physical dc-link part with/without massive energy storage equipment [21]. Usually, for the former, a bulky dc-link capacitor is needed. Therefore, such a DVR may have high cost and weight, which are undesirable for volume-critical applications [26, 27]. Addressing this issue, virtual rectifying and inverting ac/ac conversion technique has been proposed in [28, 29]. However, eight active switches are needed in the single-phase system and a complex controller should be elaborated. What's more, a transformer is required to inject the compensating voltage. In [30], a transformer-less DVR based on a buck-boost converter has been proposed. It has the benefits of compact structure and light weight. However, due to the employing of five bidirectional switches, this converter still suffers from the commutation problem and has a high cost.

A new DVR without an injection transformer is proposed. The proposed DVR is composed of an indirect ac/ac converter with only six unidirectional switches [31]. It is able to compensate for both the voltage sags and swells.

Additionally, no massive dc-link elements are used except for a small inductor. What's more, it has no tough commutation problem as all switches of the three-leg ac/ac converter can be turned on simultaneously, which is appreciated in the practical implementation. In the following sections, the circuit configuration of the DVR is stated firstly. Then, its operation principle and modulation strategy are introduced, followed by the developed control method. Finally, the simulations and experimental results are presented to verify the effective operation of the proposed topology.

## 2. Circuit configuration

As shown in Fig. 1, the proposed DVR is made up of a three-leg ac/ac converter with its output capacitor  $C_{inj}$  being in series with the grid line. SBY paralleled with  $C_{inj}$  is a by-pass switch.  $Z_o$  denotes the load impedances.  $u_g$  and  $u_o$  indicate the grid voltage and the load voltage, respectively. The other parts of the ac/ac converter consist of three legs (A, B, C), an intermediate inductor  $L$  and an input filter ( $L_g, C_g$ ). Each of the three legs (A, B, C) is composed of two switching units. Also, the switching unit can be realised by a reverse blocking-insulated-gate bipolar transistor (IGBT) or the series combination of a metal-oxide semiconductor field effect transistor/IGBT and a fast recovery diode. Under normal conditions, no compensation voltage is needed. Therefore, the by-pass switch SBY is turned on and the DVR will be in the standby status. When a voltage disturbance occurs, SBY will be turned off and the output capacitor  $C_{inj}$  is inserted in the grid line.

To mitigate voltage sag/swell, a required compensation voltage ( $u_{inj}$ ) should be generated by the DVR to recover the load voltage to pre-fault value. According to Fig. 1, the injection voltage ( $u_{inj}$ ) can be expressed as

$$u_{inj} = u_g^* - u_g$$

where  $u_g^*$  is the desired grid voltage.

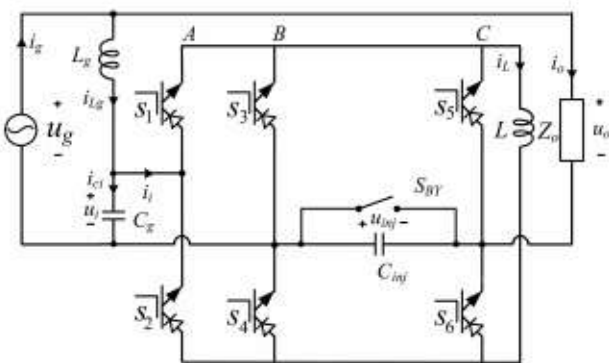


Fig. 1 Proposed topology

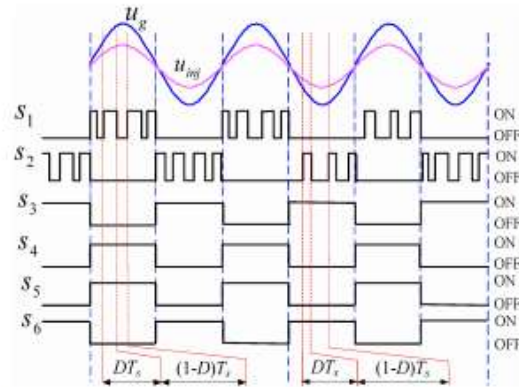


Fig. 2 Modulation strategy for voltage sag compensation

### 2.1 DVR USING Z SOURCE AC-AC CONVERTER

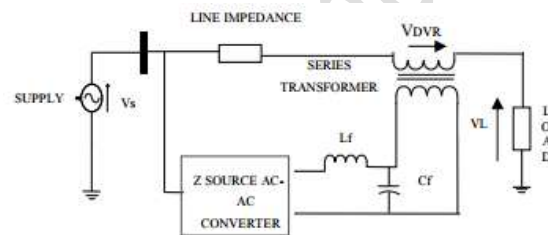


Figure 3 DVR Using Z Source AC-AC Converter

Figure 3 shows the proposed DVR using Z source AC-AC converter. It consists of Z source AC-AC converter,  $L_f C_f$  filter, Injection transformer and Load.

### 2.2 Z source AC-AC Converter

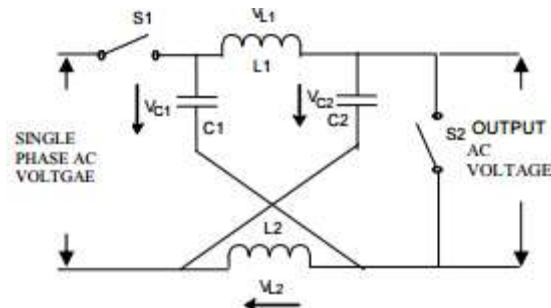


Figure 4 Z source AC- AC converter

The Z source AC-AC converter consists of two bidirectional switches and Z source network as shown in Figure 2. The Z source network consists two equal inductors  $L_1, L_2$  and two equal capacitors  $C_1, C_2$  connected in X shape. It acts as energy storage/filtering element and provides buck-boost function. Each bidirectional switches consists of two IGBTs connected in common emitter mode back to back and the two diodes provide reverse blocking capability. These two bidirectional switches are turned on and off in complement Pulse Width Modulation (PWM) signal. i.e. switch  $S_1$  is turned on with  $(D)$  and switch  $S_2$  is turned on with  $(1-D)$ . By controlling the duty ratio  $D$  the desired output voltage

can be obtained. The AC-AC converter is connected in shunt series configuration. The Z source AC-AC converter can directly convert AC voltage into AC voltage with variable amplitude. The switching frequency of PWM signal is much higher to have the smaller value of capacitor and inductor of Z source network. This converter has the following features such as the output voltage can be bucked/boosted and be in phase/out-of-phase with the input voltage reducing inrush and harmonic current. When the output voltage is boosted and in-phase with the input voltage, the DVR compensates voltage sag. When the output voltage is bucked and out of phase with the input voltage, the DVR compensates the voltage swell.

**2.3 Filter Unit**

This unit consists of inductor (L<sub>f</sub>) and capacitor (C<sub>f</sub>). It is used to reject the switching harmonics generated due to the nonlinear characteristics of switching devices. The filter can be placed either the high-voltage side or low voltage side of the injection transformer

**2.4 Injection Transformer**

The Injection / Booster transformer is a specially designed transformer to limit the coupling noise and transient energy from primary side to the secondary side. The high voltage winding is connected in series with the distribution line and the low voltage winding is connected in series with the power circuit. The basic functions of the injection transformer are : (i) It couples the injected compensating voltage generated by the AC-AC converter to the supply voltage (ii) it isolates the DVR circuit from the distribution network.

**3.OPERATION PRINCIPLE**

According to the polarities of grid voltage and injection voltage, the operation of the three-leg ac/ac converter can be classified into four modes, as listed in Table 1. Usually, the switching frequency f<sub>s</sub> is much higher than that of the input voltage. Therefore, the input power supply can be regarded as a quasi-static DC voltage in a switching period [13]. The operation principle and modulation strategy of the proposed DVR are explained in the following section.

**3.1 Voltage sag compensation**

To compensate for the voltage sags, the output voltage of the ac/ac converter (u<sub>inj</sub>) should be in phase with the grid voltage (u<sub>g</sub>). The modulation strategy for voltage sags compensation is shown in Fig. 2. As can be seen, during the positive half line cycle (u<sub>g</sub> > 0), switch S1 is driven by a high-frequency pulse-width modulation (PWM) signal, switches S2, S3, and S6 are kept being off and switches S4

and S5 are kept being on. The switching states and current paths in this operation mode are shown in Fig. 5, where the current source i<sub>o</sub> represents the load current.

**Table 1** Operation modes of the three-leg ac/ac converter

Modes	Input voltage, u <sub>g</sub>	Injection voltage, u <sub>inj</sub>	Compensation types
1	>0	>0	sag
2	≤0	≤0	sag
3	>0	≤0	swell
4	≤0	>0	swell

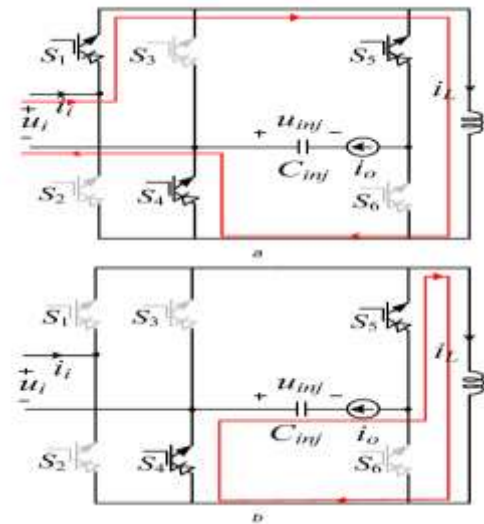


Fig.5 Switching states and current paths for voltage sag compensation when u<sub>g</sub> > 0

(a). During (0-DTs ) interval, (b) During (DTs-Ts ) interval

In the interval (0-DTs ), as shown in Fig. 5a switches S1, S4 and S5 are turned-on. However, switch S5 cannot conduct the current due to the reverse-biased voltage (u<sub>i</sub> + u<sub>inj</sub>) is imposed on it. Then the energy is transferred from the grid to the intermediate inductor and the dynamic differential equation of inductor L is

$$L \frac{di_L}{dt} = u_i$$

where u<sub>i</sub> is the voltage of filter capacitor C<sub>g</sub>, which is approximately equal to the grid voltage u<sub>g</sub> since the filter inductor L<sub>g</sub> is very small.

In the interval (DTs-Ts ), as shown in Fig. 5b, switch S1 is turned-off. Then switch S5 begins to conduct the inductor current i<sub>L</sub>, the energy stored in the intermediate inductor L is released to C<sub>inj</sub>. Applying Kirchhoff voltage laws (KVL) yields

$$L \frac{di_L}{dt} = -u_{inj}$$

Based on the volt-second balance principle, the voltage gain is derived as

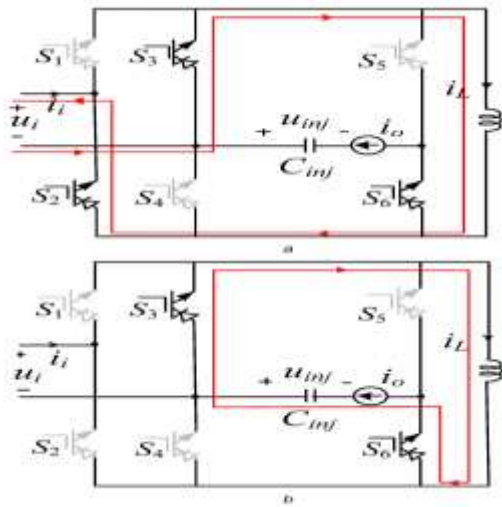


Fig.6 Switching states and current paths for voltage sag compensation when  $u_g \leq 0$

(a) During  $(0-DT_s)$  interval, (b) During  $(DT_s-T_s)$  interval

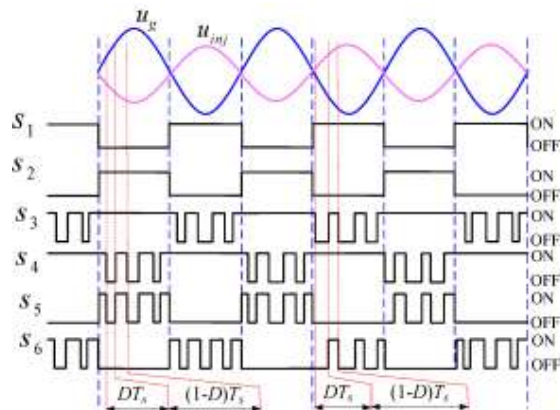


Fig. 7 Modulation strategy for voltage swell compensation

$$\frac{u_{inj}}{u_i} = \frac{D}{1-D}$$

where  $D$  is the steady-state duty cycle, which is used to adjust the amplitude of the voltage  $u_{inj}$ . Note that switch  $S_5$  is always turned on, a path for intermediate inductor current always exists. Therefore, no open-circuit will happen and the commutation problem is avoided effectively. During the negative half line cycle ( $u_g \leq 0$ ), as shown in Fig. 2, switch  $S_2$  is driven by a high-frequency pulse signal with the duty cycle  $D$ , switches  $S_1$ ,  $S_4$ , and  $S_5$  are kept being off and switches  $S_3$  and  $S_6$  are kept being on. The current paths when  $S_2$  is turned-on/ turned-off are shown in Figs. 4a) and b, respectively. The operation

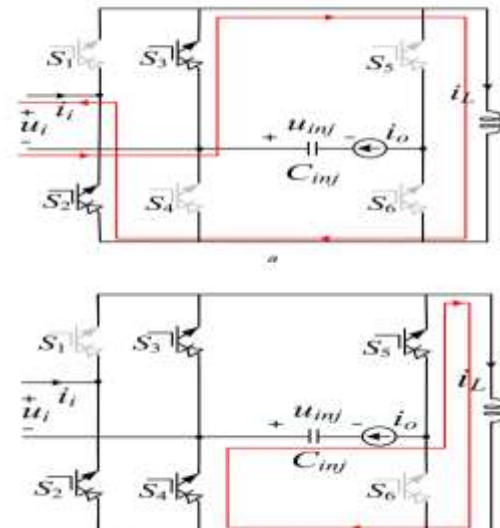


Fig. 8 Switching states and current paths for voltage swell compensation when  $u_g > 0$  (a) During  $(0-DT_s)$  interval, (b) During  $(DT_s-T_s)$  interval

processes under this situation are similar to that when  $u_g > 0$  and its voltage transfer ratio is also  $D/(1-D)$ .

### 3.2 Voltage swell compensation

To compensate for the voltage swells, the output voltage of the ac/ac converter ( $u_{inj}$ ) should be out of phase with the source voltage ( $u_g$ ). The modulation strategy with the corresponding PWM signals is shown in Fig. 7.

During the positive half line cycle ( $u_g > 0$ ), switches  $S_4$  and  $S_5$  are driven by high-frequency PWM signals, switches  $S_1$  and  $S_6$  are kept being off and switches  $S_2$  and  $S_3$  are kept being on. The switching states and current paths in this mode are shown in Fig. 8.

During the interval  $(0-DT_s)$ , as shown in Fig. 8a, switches  $S_2$  and  $S_3$  conduct the current  $i_L$ . The energy stored in the inductor is released to the grid and the dynamic differential equation of the inductor  $L$  is

$$L \frac{di_L}{dt} = -u_i$$

uring the interval  $(DT_s-T_s)$ , switches  $S_4$  and  $S_5$  are turned-on. Although switches  $S_2$  and  $S_3$  are still turned on, they will not conduct the current due to the imposed reverse-biased voltage  $u_i$  ( $|u_o|$ ). Then switches  $S_4$  and  $S_5$  begin to conduct the current  $i_L$ , as shown in Fig. 6b. The intermediate inductor  $L$  is charged by  $C_{inj}$ . Applying KVL yields

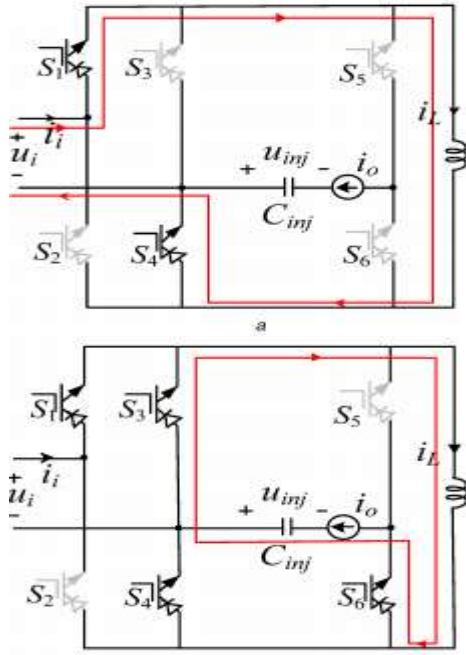


Fig.9 Switching states and current paths for voltage swell compensation when  $u_g \leq 0$  (a) During (0-DTs) interval, (b) During (DTs-Ts) interval

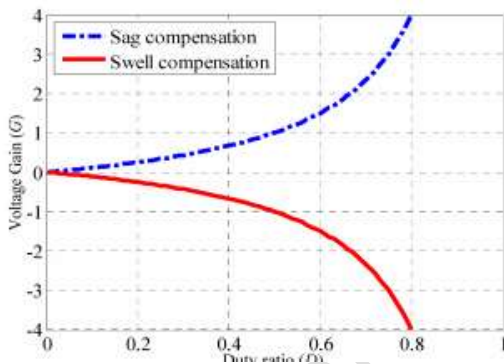


Fig.10 Voltage gain versus duty ratio for different voltage compensations

$$L \frac{di_L}{dt} = -u_{inj}$$

Therefore the voltage transfer ratio can be expressed as

$$\frac{u_{inj}}{u_i} = -\frac{D}{1-D}$$

where the sign ‘-’ means that  $u_{inj}$  is out of phase with  $u_i$ .

As can be seen, the switches S1 and S2 are always turned on, a path for intermediate inductor current always exists. Therefore, similar to voltage sag compensation, no

open-circuit will happen and the commutation problem is avoided.

During the negative half line cycle ( $u_g \leq 0$ ), switches S3 and S6 are driven by a PWM signal with a duty cycle D, switches S2 and S5 are kept being off while switches S1 and S4 are kept being on. The current paths when S3 and S6 are turned-on/turned-off are shown in Figs. 7a) and b, respectively. The operation processes are similar to those when  $u_g > 0$  and its voltage transfer ratio is also  $-D/(1-D)$ .

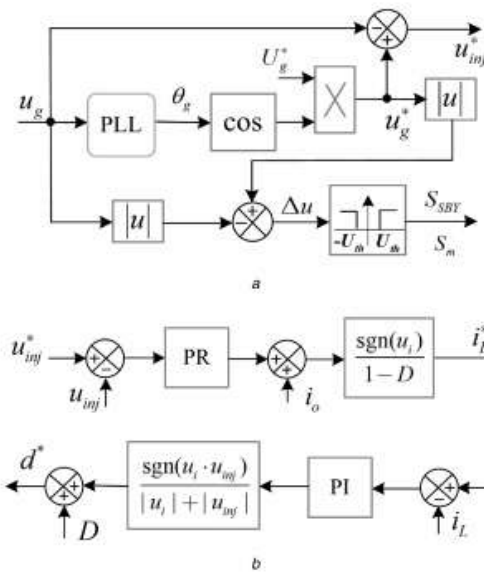


Fig. 11 Block diagram of the control scheme (a) Injection voltage reference, mode change, and start signals generation, (b) Injection voltage regulation

According to (5) and (8), the voltage gain versus duty ratio of the proposed converter for different voltage compensations is plotted in Fig. 10. As seen, the voltage gain of the DVR can be positive or negative depending on the compensation style. What's more, a wide range of voltage compensation is achieved as the proposed DVR can both buck and boost the input voltage.

### 3.3 OPEARTION OF DVR

This proposed DVR operates in the following three modes based on the magnitude of error voltage.

#### 1) Injection mode

The DVR operates in this mode as soon as the voltage sag/swell is detected. In case of voltage sag, the DVR injects an equal positive voltage which is in phase with the supply

voltage. In case of swell, the DVR injects an equal negative voltage which is antiphase with input voltage.

## 2) Standby mode

The DVR operates in this mode when the supply voltage has no voltage sag / swell. In this mode, the DVR may inject small voltage to compensate the fault

## 3) protection mode

If the current on load side exceeds a limit due to short circuit on the load, the DVR will be isolated from the system by using the bypass switches

The three phase dynamic voltage restorer consists of two circuits; one is the power circuit and other one is the control circuit. The power circuit consists of power transformer with the rating of 1KVA on each phase. These 1KVA transformers are step up transformers and are center tapped with rating 12/220V AC. These transformers are also known as booster transformers or series injection transformer because they are used to inject the restoring voltage in the line if voltage sag occurs in a system due to a fault. The other part of the power circuit is the MOSFET Inverter circuit. The inverter circuit consist of six 8×8 Array for current boosting on the 12V primary side of the series injection transformers. Two 8×8 arrays are connected per phase to the 12V side of each 1KVA transformer. This inverter module is connected to an external energy source which is a DC 12V battery in this case. The inverter module is used to convert the DC to AC voltage. The inverter topology used here is the half bridge VSI topology. For a single phase operation i.e. red phase MOSFET B1 is turned on for positive half cycle and the switch B2 is turned on for the negative half cycle. One of the switches conducts at a time. If u consider the three phase operation with a three phase load than topology used is named as 6 leg DC to AC voltage source inverter topology.

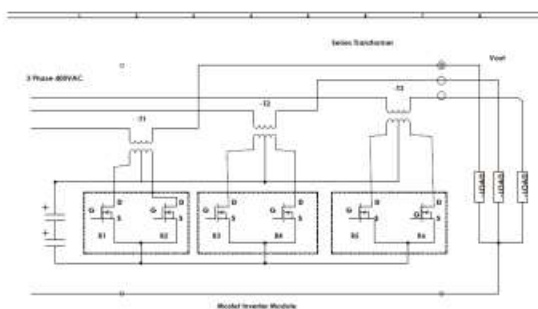


Figure 12: Power circuit of three phase DVR

## 4. Simulations and experimental results

### 4.1 Simulation results

A simulation study was conducted in Matlab/Simulink environment with the circuit parameters listed in Table 2. The simulation results under both voltage sag and swell conditions are shown in Figs. 13 and 14, respectively.

**Table 2** Parameters used in simulations and experiments

Parameters	Symbol	Value
load capacity	$P_o$	250 W
load voltage	$v_o$	110 V <sub>rms</sub>
load angular frequency	$\omega_l$	314 rad/s
input filters	$L_g/C_g$	0.6 mH/10 $\mu$ F
intermediate inductor	$L$	500 $\mu$ H
output filters	$C_{inj}$	5 $\mu$ F
load	$R$	50 $\Omega$
switching frequency	$f_s$	20 kHz

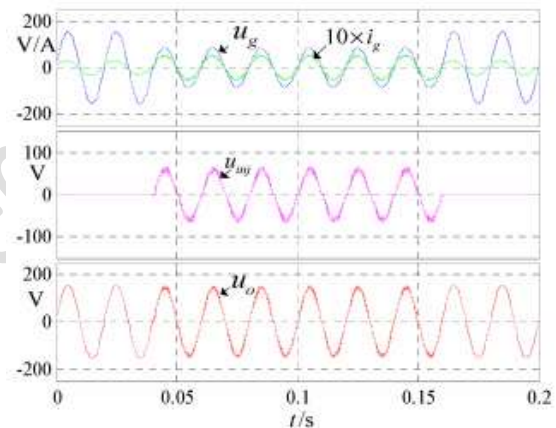


Fig. 13 Simulation results for sag compensation

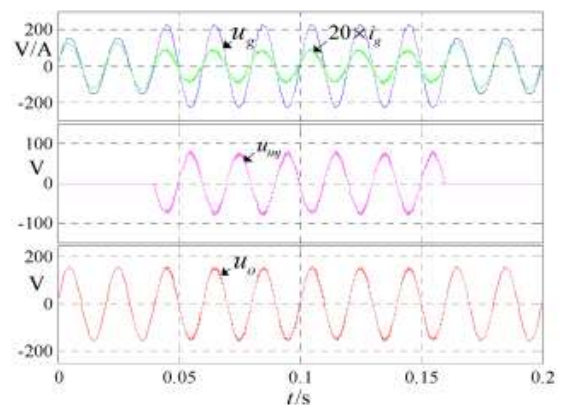


Fig. 14 Simulation results for swell compensation

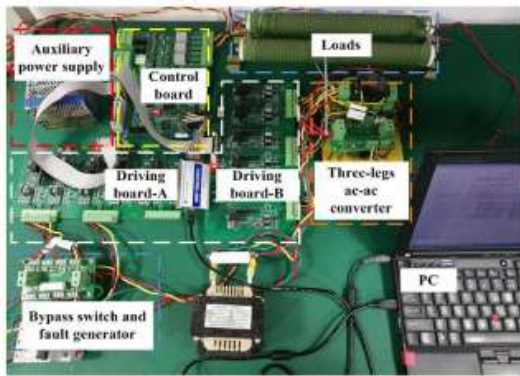


Fig. 15 Experimental setup for the converter

Fig. 13 shows the simulation results for the DVR under voltage sag conditions. As can be seen, the magnitude of the grid voltage decreases from  $110\sqrt{2}$  to  $60\sqrt{2}$  V 0.04 s and recovers to  $110\sqrt{2}$  V at 0.16 s. During this period, a required voltage, in phase with the grid voltage, is generated by the DVR and injected into the grid line. Therefore, the load voltage remains at its desired value. In other intervals, the grid voltage is at the rated value. So, the DVR is in a standby state and no compensation voltage is generated. The simulation results for the DVR under voltage swell condition are shown in Fig. 14. The magnitude of the grid voltage increases from  $110\sqrt{2}$  to  $60\sqrt{2}$  V at 0.04 s and recovers to  $110\sqrt{2}$  V at 0.16 s. During this period, a compensation voltage  $u_{inj}$  with the magnitude of  $50\sqrt{2}$  V is provided by the DVR, and it is out of phase with the grid voltage. Therefore, the load voltage can remain unchanged during the voltage swell disturbance.

#### 4.2 Experimental results

A prototype for the proposed converter was built in the lab as shown in Fig. 15 for experimental verification. The setup includes the three-leg ac-ac converter, driving boards A and B, auxiliary power supply, control board (with a signal processor TMS320F28335), bypass switch and voltage disturbance generator. The experimental parameters are the same as those in the simulation. The experimental results for sag and swell compensations are shown in Figs. 14 and 15, respectively. The waveforms of grid voltage ( $u_g$ ) and current ( $i_g$ ), injection voltage ( $u_{inj}$ ) and load voltage ( $u_o$ ) for voltage sag compensation are presented in Fig. 14a. As can be seen, when a 30% voltage sag is applied to the grid voltage, a proper injection voltage is generated immediately and the load voltage is fully maintained at the nominal value, which demonstrates the effectiveness of the compensator. In Fig. 14b, the source voltage and PWM signals of the switches  $S_1$ ,  $S_4$  and  $S_5$  are depicted. The driving signals of the switches  $S_4$  and  $S_5$  are modulated to remain at a high level during the positive half cycle of the grid voltage. Therefore, the open circuit of the intermediate

inductor current can be avoided, which offers a simple and reliability operation processes.

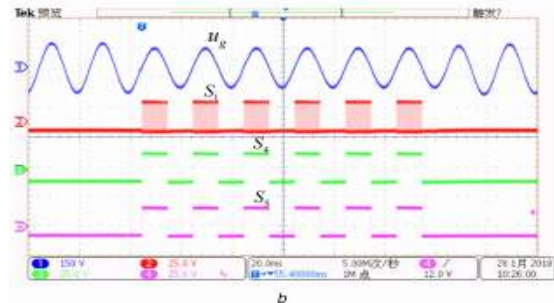
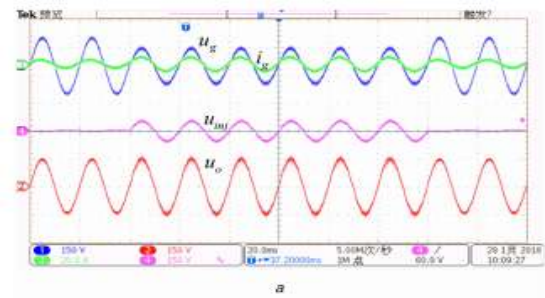


Fig. 16 Experimental results for sag compensation

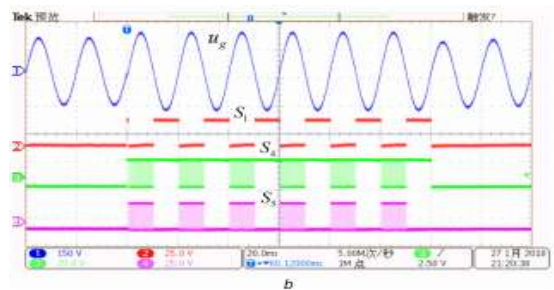
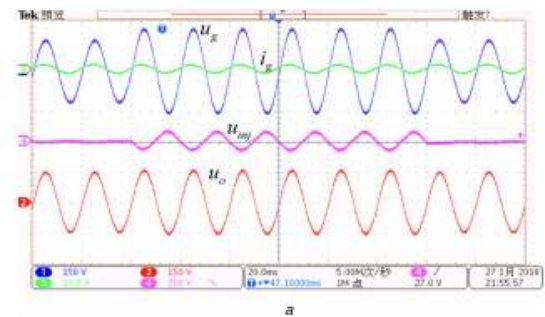


Fig.17 Experimental results for swell compensation

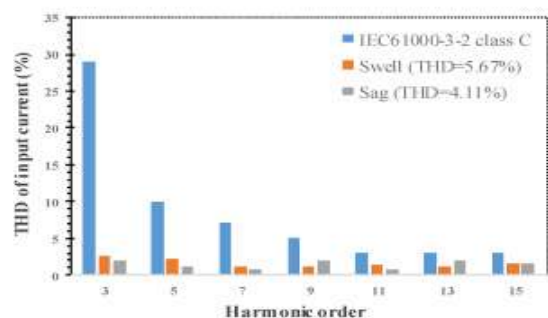


Fig. 18 Measured input current harmonics under sag and swell compensation

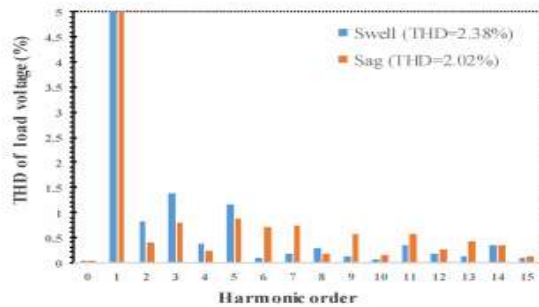


Fig.19 Measured load voltage harmonics under sag and swell compensation

In Fig. 17a, the waveforms of grid voltage ( $u_g$ ) and current ( $i_g$ ), injection voltage ( $u_{inj}$ ) and load voltage ( $u_o$ ) during the voltage swell period are presented. A 30% voltage swell in the amplitude of grid voltage is generated. The load voltage remains unchanged since a proper injection voltage has been provided by the restorer. Fig. 17b shows the grid voltage interruptions and modulation PWM signals of the switches S1, S4, and S5 during this period. Input current harmonics (up to 15th) of the restorer under sag and swell compensations are shown in Fig. 18. As can be seen, it can meet IEC-61000-3-2 class C limit with a margin. The total harmonic distortion (THD) of input current is 4.11% and 5.67% at voltage sag and swell compensation, respectively. THDs of the load voltage are plotted in Fig. 19. It shows that the restorer has a low-voltage harmonics under different voltage disturbances (sag and swell). In sum up, the proposed DVR has a good PQ at both the input and output.

## 5.CONCLUSION

A DVR based on the three-leg ac/ac converter is proposed. It can be used to restore the load voltage in both voltage sag and swell conditions. Since no injection transformer and bulky dc-link elements are required, it has a compact structure, small volume, and light weight. Moreover, the commutation problem is effectively avoided. A laboratory prototype is built to verify the theoretical analysis. In short, the proposed DVR can be a good candidate for compensating voltage disturbances, due to its high reliability and low costs.

## REFERENCES

[1] Chan, J.Y., Milanovi, J.V.: 'Assessment of the economic value of voltage sag mitigation devices to sensitive industrial plants', IEEE Trans. Power Deliv., 2015, 30, (6), pp. 2374–2382

[2] Trindade, F.C.L., Nascimento, K.V.D., Vieira, J.C.M.: 'Investigation on voltage sags caused by DG anti-islanding protection', IEEE Trans. Power Deliv., 2013, 28, (2), pp. 972–980

[3] IEEE Recommended Practice for Monitoring Electric Power Quality, IEEE Standard 1159-2009. (IEEE, New York, USA, 2009)

[4] Barros, J.D., Silva, J.F.: 'Multilevel optimal predictive dynamic voltage restorer', IEEE Trans. Ind. Electron., 2010, 57, (8), pp. 2747–2760

[5] Massoud, A.M., Ahmed, S., Enjeti, P.N., et al.: 'Evaluation of a multilevel cascaded-type dynamic voltage restorer employing discontinuous space vector modulation', IEEE Trans. Ind. Electron., 2010, 57, (7), pp. 2398–2410

[6] E. Babaei, M. F. Kangarlu, M. Sabahi, "Mitigation of Voltage Disturbances Using Dynamic Voltage Restorer Based on Direct Converters", IEEE TRANSACTIONS ON POWER DELIVERY, Vol. 25, No. 4, October 2010.

[7] M. T. Ali, F. Abbas, A. Nadeem M. Yaqoob, S. M. Malik, M. J. Iqbal, "Effect of PI Controller on Efficiency of Dynamic Voltage Restorer for Compensation of Voltage Quality Problems", 16th International Power Electronics and Motion Control Conference and Exposition, Antalya, Turkey 21-24 Sept 2014.

[8] R. Kalaivani, K. Arunvishnu, M. G. J. Hussein, R. Lokeshwaran, M. Rajkumar, "Elimination of Voltage Sag/Swell using Dynamic Voltage Restorer", International Journal for Research in Technological Studies, Vol. 3, Issue 4, March 2016.

[9] D. Murali, Dr. M. Rajaram, "Simulation and implementation of DVR for Voltage Sag compensation", Vol. 23- No.25, June 2011.

[10] M. T. Ali, Z. Jianhua, M. Yaqoob, F. Abbas, S. F. Rafique, "Design of an Efficient Dynamic Voltage Restorer for Compensating Voltage Sags, Swells, and Phase Jumps", 16th International Power Electronics and Motion Control Conference and Exposition Antalya, Turkey 21-24 Sept 2014.

## AUTHOR'S PROFILE:



[1]. **S.RAMA LAKSHMI**  
Pursuing her Masters Degree in Department of EEE from Kakinada Institute Of Technological Sciences (Kits), Ramachandrapuram.

[2]. **PUVVULA HEMANTH PRITHVI**, Completed his B.Tech and M.Tech Degrees from Aditya Engineering College, Surampalem. Presently he is working as Assistant Professor in Department of EEE, KITS College , Ramachndrapuram. His Interested Area is Power Electronics.

Journal of Engineering Sciences